Published in final edited form as:

Am J Surg Pathol. 2017 January ; 41(1): 12–24. doi:10.1097/PAS.0000000000000721.

Novel High-Grade Endometrial Stromal Sarcoma: A Morphologic Mimicker of Myxoid Leiomyosarcoma

Lien N. Hoang[1], **Amandeep Aneja**[1], **Niamh Conlon**[2], **Deborah F. Delair**[1], **Sumit Middha**[1], **Ryma Benayed**[1], **Martee L. Hensley**[3], **Kay J. Park**[1], **Travis J. Hollmann**[1], **Meera R. Hameed**[1], **Cristina R. Antonescu**[1], **Robert A. Soslow**[1,*], and **Sarah Chiang**[1,*]

[1]Department of Pathology, Memorial Sloan Kettering Cancer Center, New York, NY, USA
[2]Department of Pathology, Cork University Hospital, Wilton, Cork, Ireland [3]Gynecologic Medical Oncology Service, Department of Medicine, Memorial Sloan Kettering Cancer Center, Weill Cornell Medical College, New York, NY, USA

Abstract

Endometrial stromal sarcomas (ESS) are often underpinned by recurrent chromosomal translocations resulting in the fusion of genes involved in epigenetic regulation. To date, only *YWHAE-NUTM2* rearrangements are associated with distinctive high-grade morphology and aggressive clinical behavior. We identified 3 ESS morphologically mimicking myxoid leiomyosarcoma of the uterus and sought to describe their unique histopathologic features and identify genetic alterations using next-generation sequencing. All cases displayed predominantly spindled cells associated with abundant myxoid stroma and brisk mitotic activity. Tumors involved the endometrium and demonstrated tongue-like myometrial infiltration. All 3 were associated with an aggressive clinical course, including multisite bony metastases in 1 patient, progressive peritoneal disease after chemotherapy in another and metastases to the lung and skin in the last patient. All 3 ESS were found to harbor *ZC3H7B-BCOR* gene fusions by targeted sequencing and fluorescence in situ hybridization. On the basis of the review of these cases, we find that ESS with *ZC3H7B-BCOR* fusion constitutes a novel type of high-grade ESS and shares significant morphologic overlap with myxoid leiomyosarcoma.

Keywords

endometrial stromal sarcoma; uterine sarcoma; *ZC3H7B*; *BCOR*; translocation; myxoid leiomyosarcoma; polycomb repressor complex

Corresponding Author: Robert A. Soslow, MD, Memorial Sloan Kettering Cancer Center, Department of Pathology, 1275 York Ave, New York, NY 10065, United States, Phone: (212) 639-5905, Fax: (646) 422-2070, soslowr@mskcc.org.
*Co-principal investigators

The authors have no conflicts of interest to disclose.

Introduction

Endometrial stromal sarcomas (ESS) account for 1% of all uterine malignancies and 15% of malignant mesenchymal neoplasms of the uterus.[1] Since the foundational descriptions provided by Norris and Taylor in 1966, the classification of ESS has undergone several modifications.[2–5] Currently, the 2014 World Health Organization categorizes ESS into low-grade ESS (LG-ESS), high-grade ESS (HG-ESS), and undifferentiated uterine sarcoma (UUS).[6]

Morphologically, LG-ESS resembles proliferative-type endometrial stroma.[2] It is composed of monotonous populations of small cells with round, oval to fusiform nuclei concentrically arranged around thin-walled spiral arterioles.[2,7,8] Tongue-like infiltration of the myometrium and “worm-like” plugs in the uterine vessels are characteristic findings. Collagen plaques, cholesterol clefts, and foamy histiocytes may also be present.[8] Mitotic activity is usually <5/10 high power fields (HPF); however higher mitotic indices may be encountered.[7–9] A myriad of variant histologic features have been described, including smooth muscle, glandular, sex-cord, and rhabdomyoblastic differentiation, as well as myxoid/fibromyxoid, fibrous, pseudopapillary, and epithelioid change.[7,10–21] By immunohistochemistry, LG-ESS is positive for estrogen receptor (ER), progesterone receptor (PR), and CD10.[22–24] Approximately half of LG-ESS harbor t(7;17) chromosomal translocations resulting in *JAZF1-SUZ12* gene fusion.[25–27] Other gene fusions, including *JAZF1-PHF1*[28], *EPC1-PHF1*[28], *MEAF6-PHF1,*[29,30], and *MBTD1-CXorf67*[31] are rare. While *PHF1* rearrangements have been reportedly associated with sex-cord differentiation[32], other gene fusions found in LG-ESS have not been linked with variant morphologic features. *JAZF1-SUZ12* gene fusions are only extraordinarily encountered in the fibromyxoid variant.[13] LG-ESS tend to be indolent tumors with 5-year survival rates >90% for low-stage disease.[7,33]

UUS is considered a diagnosis of exclusion and harbors little histologic resemblance to normal endometrial stroma, particularly when the nuclei are pleomorphic.[6] The tumor cells in UUS of the pleomorphic type display severe nuclear atypia, brisk mitotic activity, and necrosis. Most reported UUS exhibit complex karyotypes without defining genetic rearrangements and portend a dismal prognosis.[34–36]

The term, HG-ESS, was recently reintroduced into the classification of endometrial stromal tumors based on the discovery of the t(10;17) translocation resulting in fusion of *YWHAE* and *NUTM2* genes. *YWHAE*-rearranged HG-ESS is characterized by a proliferation of round cells with nested or pseudoglandular patterns separated by thin-walled vessels. The nuclei of the round cells are larger and display more irregular nuclear contours compared to LG-ESS and share morphologic overlap with UUS of uniform type.[26,37] Mitotic activity is >10/10 HPF, and necrosis is common. Approximately half of reported cases are admixed with a low-grade fibromyxoid component which expresses ER, PR, and CD10. In contrast, the round cell component is usually negative for these markers, but is often strongly and diffusely positive for cyclin D1 and CD117.[38,39] *YWHAE*-rearranged HG-ESS bear an intermediate prognosis, between LG-ESS and UUS.[37]

Although rare, morphologically HG-ESS and UUS of uniform type that lack *YWHAE*-rearrangements exist and likely harbor genetic alterations that have yet to be characterized.[40] Here we describe a novel form of high-grade ESS exhibiting aggressive clinical behavior as well as histologic and immunophenotypic features mimicking myxoid leiomyosarcoma (LMS). In this study, we detail the unusual and distinct morphology of this tumor. We performed next-generation sequencing and fluorescence in situ hybridization to uncover genetic alterations that underpin this tumor type.

Materials and methods

Case selection

From 2013 to 2016, 3 uterine sarcomas displaying morphologic overlap between ESS and myxoid LMS were identified on the Gynecologic Pathology Consultation Service at Memorial Sloan Kettering Cancer Center, New York, NY. Available hematoxylin and eosin stained and immunohistochemical-stained slides from the original institutions were reviewed to delineate the morphologic and immunophenotypic features. Clinical data were reviewed for demographics, presentation, treatment, and outcome.

Next Generation Sequencing

For case 1, genomic alterations were profiled using MSK-IMPACT (Memorial Sloan Kettering – Integrated Mutation Profiling of Actionable Cancer Targets)[41], a custom hybrid capture-based sequencing assay, performed on formalin-fixed paraffin-embedded (FFPE) tumor tissue. Custom oligonucleotide probes were designed to capture all exons and selected regulatory regions and introns of 410 key cancer genes. Captured pools from paired normal and tumor samples were sequenced on an Illumina HiSeq2500, with a minimum depth of coverage of 100X. Variants were called with reference to the patient's matched normal sample, to assure they were all somatic in nature. Tumor DNA of case 2 was subjected to Foundation One sequencing assay (http://www.foundationone.com), which targeted the exons of 315 cancer-related genes and introns from 28 genes often rearranged or altered in cancer on an Illumina HiSeq2000. The tumor from case 3 was analyzed using the MSK-Solid Fusion assay, a targeted RNA-based panel that utilizes the Archer Anchored Multiplex PCR (AMP™) technology[42] and next-generation sequencing to detect genes fusions in solid tumor and sarcoma samples. Unidirectional gene specific primers were designed to target specific exons in 35 genes known to be involved in chromosomal rearrangements, RNA was extracted from tumor FFPE material followed by cDNA synthesis and library preparation. Final targeted amplicons were sequenced on an Illumina MiSeq. Data was analyzed using the Archer™ Software (version 4.0.10).

Fluorescence In Situ Hybridization

Fluorescence in situ hybridization (FISH) was performed on interphase nuclei from FFPE 4 μm tissue sections from cases 1 and 2 as previously described.[43] Custom probes using bacterial artificial chromosomes (BAC) covering and flanking the *BCOR* gene and *ZC3H7B* gene were chosen according to the UCSC genome browser (http://genome.ucsc.edu). The BAC clones were retrieved from BACPAC sources of the Children's Hospital of Oakland Research Institute (CHORI) (Oakland, CA) (http://bacpac.chori.org). The DNA from

individual BACs were isolated according to manufacturer's recommendations, labelled with different fluorochromes in a nick translation reaction, denatured, and then hybridized to pretreated slides. The slides were then incubated, washed, and mounted with DAPI in an anti-fade solution, as previously reported.[44] The genomic location of each BAC set was confirmed by hybridizing them to normal metaphase chromosomes. Using a Zeiss fluorescence microscope (Zeiss Axioplan, Oberkochen, Germany), 200 successive nuclei were examined, controlled by Isis 5 software (Metasystems). A positive score was given when at least 20% of the nuclei displayed a break-apart signal. Nuclei with incomplete sets of signals were omitted from interpretation.

Results

Clinicopathologic Features

Case 1—A 36-year-old gravida 2 para 1 woman with a history of fibroid uterus presented with increasing pelvic pain. An ultrasound revealed that her fibroids had increased in size compared to 2 years prior, and she underwent a myomectomy with morcellation and removal of tissue measuring up to 15 cm in aggregate. A pathologic diagnosis of sarcoma was rendered, and a completion hysterectomy, bilateral salpingo-oophorectomy, omentectomy, and debulking were subsequently performed 1 month later. Intraoperatively, a large heterogeneous mass attached to the uterus as well as extensive infiltration of the mesentery were found. All gross disease was completely resected.

On histopathologic examination, a 10 cm gray-white hemorrhagic tumor was present in the uterine fundus with extension into the cervix and metastases to the right adnexae and omentum. The tumor was predominantly spindled with minor epithelioid areas, had focal fascicular architecture, and extensive myxoid change. The cells displayed round to oval nuclei with irregular nuclear contours, inconspicuous nucleoli, and hyperchromatic to clear chromatin (Figure 1). The tumor edge displayed broad pushing and infiltrative growth patterns, with the latter predominating. There were delicate thin-walled capillaries, although tumor cells did not whorl around them (Figure 2). Mitotic activity was 3–4/10 HPF and reached 10/10 HPF in 1 slide. Ki-67 proliferation index was 20%. The tumor was diffusely positive for CD10, ER, and PR, and focally positive for SMA, while negative for desmin and ALK1. "Invasive endometrial stromal neoplasm, with features between low-grade and high-grade" was diagnosed at the original institution. Two independent external consultations rendered a diagnosis of myxoid LMS.

The patient received postresection whole-pelvic radiation and was treated with an aromatase inhibitor. Twenty-two months after the myomectomy, the patient developed peritoneal disease, implants on the surface of the liver, and a lytic lesion of the sacrum. She was treated with a change in the aromatase inhibitor and stereotactic radiosurgery to the sacral lesion. Six months later, she developed multisite bony metastases, increasing peritoneal disease and enlarged pelvic lymph nodes. Treatment was changed to cytotoxic chemotherapy with gemcitabine plus docetaxel. There was progression of disease after 2 cycles of therapy. The patient was then treated with doxorubicin.

Case 2—A 48-year-old gravida 3 para 1 woman with a history of fibroid uterus noticed increased vaginal bleeding and pelvic pain for 5 months despite leuprolide therapy. She underwent a planned laparoscopic hysterectomy for presumed fibroids. In the operating room, significant bleeding was noted due to gross rupture of a large pelvic mass involving the anterior uterus, left adnexa, broad ligament, and surrounding structures. The procedure was converted to open total abdominal hysterectomy, bilateral salpingo-oophorectomy, and debulking surgery.

Histopathologic examination revealed a 12 cm yellow-tan exophytic tumor in the fundus, transmurally involving the uterine wall, as well as the left adnexa, parametrium, pelvic side wall, small bowel, and a para-aortic lymph node. The tumor was composed of spindled cells with areas of fascicular architecture and myxoid change (Figure 3). The tumor was focally hypercellular in the less myxoid areas and demonstrated tongue-like myometrial invasion with worm-like plugs of tumor within blood vessels. The tumor nuclei displayed irregular nuclear contours, inconspicuous nuclei, and hyperchromatic to clear chromatin. Abundant mitotic activity (>30/10HPF), atypical mitotic figures, and thin-walled vessels were present, but lacked whorling of tumor cells (Figure 4). By immunohistochemistry, the tumor cells were diffusely positive for CD10, focally positive for desmin and negative for ER, PR, caldesmon, SMA, ALK1, cyclin D1, inhibin, S100, GFAP, and AE1/AE3. Alcian Blue was diffusely positive. While the tumor was noted to have features resembling both ESS and myxoid LMS, a diagnosis of UUS was ultimately rendered at the original institution.

CT imaging performed 2 months after resection showed recurrent pelvic masses. She was treated with doxorubicin plus ifosfamide, with at best stable disease on follow-up imaging.

Case 3—A 44-year-old gravida 4 para 1 woman presented with vaginal bleeding. She had a cervical polypectomy and endometrial curettings which revealed fragments of sarcoma most consistent with LMS. Two external consultations from 2 separate institutions diagnosed myxoid LMS. The patient then had a hysterectomy, bilateral salpingo-oophorectomy, and hypogastric lymph node excised.

On histopathologic examination, there was a 2.5 cm tumor in the uterine corpus and 0.7 cm nodule in the cervix, diagnosed as a myxoid LMS. The tumor was composed of spindled cells in a background of myxoid stroma (Figures 5 and 6). There were both tongue-like and infiltrative patterns of invasion into the myometrium. The nuclei were enlarged, had irregular nuclear contours, hyperchromasia, coarse chromatin, and inconspicuous nucleoli. Scattered thin walled blood vessels were present. The mitotic count was 10/10 HPF. Worm-like lymphovascular invasion was also present.

The patient received gemcitabine and docetaxel. Ten months after the initial diagnosis, the patient developed multiple lung metastases. A fine-needle aspiration biopsy was performed revealing a spindle cell neoplasm, favored to be metastatic myxoid LMS from the uterine primary. The tumor was positive for CD10, SMA, and negative for desmin, caldesmon, ER, PR, CD34, and S100. She was treated briefly with single agent gemcitabine but stopped treatment due to poor tolerance. Over the next 2 years, some lung lesions demonstrated a slow increase in size while others remained stable or regressed. Radiofrequency ablation was

given to several of the lung lesions. Two years later, the patient had progression of disease involving thoracic and pelvic lymph nodes, while the small lung metastases remained stable. She was treated with liposomal doxorubicin and had a minor radiographic response. One year later, the right upper lobe mass grew to obstruct the right mainstem bronchus, and she was treated with palliative radiation to the mass. Further progression of disease in the pelvis involved the sacral plexus, and the patient developed a large, symptomatic deep venous thrombosis, treated with a venous stent and anticoagulation. Subsequently, the patient developed a non healing skin lesion involving the right temple. A biopsy demonstrated a malignant spindle cell neoplasm showing focal weak staining for S100 and diffuse positivity for p75-NGFR and vimentin, while lacking MelanA, tyrosinase, and SMA expression. On the basis of the tumor location and immunophenotype, a malignant spindle cell melanoma was diagnosed at the original institution. Additional stains performed at our institution showed diffuse staining for cyclin D1, focal staining for SMA and SOX10 (focal weak), but no desmin or BRAFV600E staining. This immunoprofile prompted comparison with the prior uterine and lung masses. On the basis of morphologic similarity among all three tumors, a cutaneous metastasis of the patient's known widely metastatic uterine sarcoma was ultimately confirmed at our institution.

Next-Generation Sequencing

Case 1 was subjected to MSK-IMPACT sequencing at a median sequencing depth of coverage of 924X and was found to have an in frame fusion between *ZC3H7B* exon 10 (NM_017590) and *BCOR* exon 7 (NM_001123385) (t(X;22)(p11.4;q13.2)(chrX:c.3146::chr22:c.1525)) (Figure 7). No somatic mutations, copy number aberrations, or other structural rearrangements were identified. Genomic testing of case 2 by Foundation One also revealed a *ZC3H7B-BCOR* fusion in addition to amplification of *CDK4*, *MDM2*, *FRS2* genes, *HDAC4-HABP2* fusion, and seven variants of unknown significance. Case 3 was analyzed using the MSK-Solid Fusion panel. This also revealed an in-frame fusion between *ZC3H7B* exon 10 (NM_017590) and *BCOR* exon 7 (NM_001123385).

Fluorescence In Situ Hybridization

In cases 1 and 2, FISH confirmed gene rearrangements in both *ZC3H7B* and *BCOR* (Figure 8).[43] FISH for *YWHAE* and *JAZF1* rearrangements were also performed on case 2 at the original institution and were both negative by report.

Discussion

In this report, we describe for the first time the association of *ZC3H7B-BCOR* fusion resulting from t(X;22)(p11.4;q13.2) in tumors with extensive myxoid change and focal fascicular architecture mimicking myxoid LMS and thus representing a potential diagnostic pitfall. Two cases were misdiagnosed as myxoid LMS, including 1 case in which the unusual skin recurrence and immunophenotype (limited S100 and SOX10 positivity and diffuse p75-NGFR positivity) also misled to a new primary diagnosis of malignant melanoma. In another case, myxoid LMS was considered in the differential diagnosis. Detection of the *ZC3H7B-BCOR* fusion prompted a re-review of the histopathology of the uterine primary and recurrences, and in all cases, a diagnosis of ESS with extensive myxoid features was

ultimately rendered based on the molecular genetic findings, involvement of the endometrium, and characteristic pattern of myometrial invasion.

ZC3H7B-BCOR fusion has been previously reported in ESS by Panagopoulos *et al.* in 2013.[45] In their series, both tumors were composed of non pleomorphic spindled cells, and although not explicitly mentioned, one of them harbored a myxoid quality in the figure presented. One case had minimal mitotic activity (0 to 1/10 HPF) and expressed CD10, ER, and PR. However, the other had brisk mitotic activity (26/10 HPF) and expressed CD10, but lacked ER and PR staining. Both patients presented with high-stage disease, in which tumors metastasized to the distal ureter and bowel, respectively. No recurrences were documented at the time of publication; however the follow-up period was not specified. The morphologic and clinical features parallel those observed in our study. In a separate study by Lee *et al.*, karyotypic data available in 12 HG-ESS included 2 cases demonstrating t(X;22)(p11.4;q13.2). Although this translocation was not characterized in their study and the morphologic description of these 2 cases was not available in their report, both tumors likely harbor *ZC3H7B-BCOR* rearrangements based on their cytogenetic profiles.[34,45]

The morphologic distinction of *BCOR*-rearranged ESS from myxoid LMS poses an important diagnostic challenge. Myxoid LMS can also exhibit spindled cells with fascicular architecture, nonpleomorphic nuclei and minimal mitotic activity.[46–48] In contrast to myxoid LMS, however, our ESS tumors lacked long fascicles, thick-walled blood vessels, dense eosinophilic cytoplasm and cigar-shaped nuclei with blunted ends, features which typify smooth muscle neoplasms. Two tumors in our series were SMA positive, and 1 was focally desmin positive. The presence of desmin staining, however, does not exclude a diagnosis of ESS, as desmin positivity has been reported in up to 50% of ESS, especially those that demonstrate smooth muscle differentiation.[22,23] In addition, all 3 of our cases demonstrated lymph node involvement, 2 radiologically and 1 confirmed by biopsy. Although lymph node metastases in uterine sarcomas are overall rare, lymph node involvement is more frequently seen in ESS than in LMS.[49–51] All 3 patients were also alive with disease 37, 13, and 80 months, respectively, at last follow-up from the time of diagnosis, similar to the clinical course of *YWHAE*-rearranged ESS[37] rather than LMS which has a reported 66% 5-year survival rate.[50]

Given some of the overlapping morphologic features with myxoid LMS, we speculate that a subset of myxoid LMS may actually represent *BCOR*-rearranged ESS. Although it is acknowledged that CD10 is not an entirely specific marker for endometrial stromal differentiation, it is also worthwhile mentioning that in 2 of the largest series of myxoid LMS, 10/18 (55%) and 7/18 (39%) of tumors showed moderate to strong (2+ to 3+) staining for CD10, similar to our ESS.[48] The investigation for *BCOR* and *ZC3H7B* rearrangements in histologically classified myxoid LMS would be an interesting endeavour and merits further study.

Kurihara and colleagues was the first to emphasize the distinction between uniform and pleomorphic types of UUS. In their 7 cases classified as UUS of uniform type, 2 were described as having diffuse fibromyxoid features and fascicular architecture. It is, therefore, possible that these 2 cases of uniform-type UUS described by Kurihara *et al.*, and even some

of the cases previously described as fibromyxosarcoma in the uterus, may also represent *BCOR*-rearranged ESS.[26,52]

BCOR (BCL-6 interacting corepressor) can bind to the POZ domain of *BCL-6*, potentiating its function, interact with histone deacetylases, or form chromatin modifying complexes which along with the polycomb repressive complex 1 enhance transcriptional repression.[53–55] *BCOR* has also been shown to affect embryonic and mesenchymal stem cell differentiation[56,57], hematolymphoid development [58,59], and determination of laterality.[60,61] While germline mutations in *BCOR* result in the syndromic diseases, oculo-facio-cardio-dental syndrome and Lenz microphthalmia,[62] somatic *BCOR* mutations have been reported in various hematolymphoid malignancies[63–68], retinoblastoma[69], medulloblastoma [70], central nervous system primitive neuroectodermal tumors[71], rhabdomyosarcoma,[72] and clear cell sarcoma of the kidney.[73–76]

BCOR rearrangements are not limited to ESS. Recently, Antonescu *et al.* has reported *ZC3H7B–BCOR*, *MEAF6–PHF1* and *EPC1–PHF1* fusions in a subset of ossifying fibromyxoid tumors (OFMT)[43]; these genetic rearrangements have also been reported in ESS.[28,29,45] Notably, *ZC3H7B-BCOR* rearrangements were identified in 2 OFMT, both of which displayed malignant features and were S100-negative.[43] Rearrangements in *BCOR* have also been identified in undifferentiated small blue round cell tumors, undifferentiated spindle cell sarcomas that lack EWS rearrangements,[77–79] and a single case of acute promyelocytic leukemia.[80] The presence of *BCOR* rearrangements across diverse tumor types suggests the likely role of *BCOR* driving tumourigenesis. It is noteworthy that *SUZ12*, *PHF1*, and *MBTD1* are also members of the polycomb repressive complex family, and *EPC1* and *MEAF2* function to alter acetylation of histone proteins.[3,28,29] It appears that all genes found to be rearranged in ESS have a unifying role in epigenetic regulation, either through polycomb-mediated gene silencing or post-translational covalent modification of histone proteins.

Less is known about *ZC3H7B* (also known as RoXaN). It contains several domains (tetratricopeptide repeats, zinc finger motifs, LD motif) responsible for coordinating protein-protein and protein-nuclei acid interactions. It is thought to have roles in regulating translation and nucleocytoplasmic localization.[45,81,82]

In addition to myxoid LMS, a number of other entities enter the differential diagnosis for cases with a histologic appearance like the 3 ESS described here. An argument can be made that the morphology in the present 3 cases resemble the myxoid/fibromyxoid variants of LG-ESS reported in the literature.[16–19,52,83,84] Our 2 cases, however, had mitotic activity >10/10HPF (at least focally), displayed nuclear features that exceeded the level of cytologic atypia seen in LG-ESS and had no areas with prototypical LG-ESS histology. Although OFMT and our current cases of *BCOR*-rearranged ESS share some morphologic and molecular similarities, we still consider these 2 tumors as distinct entities. OFMT tend to occur in the deep soft tissues, is well circumscribed, and typically has a shell of lamellar or woven bone.[43] Inflammatory myofibroblastic tumors (IMT) may be myxoid and thus are also in the differential diagnosis, but are typically positive for ALK1 and lack the infiltrative pattern characteristic of ESS.

Immunohistochemistry has long played an important role in the distinction between endometrial stromal tumors and smooth muscle neoplasia. A panel of CD10 and 2 smooth muscle markers including desmin has been recommended in the differential diagnosis of a conventional LG-ESS or endometrial stromal nodule and a highly cellular leiomyoma. The utility of immunohistochemistry in assessing uterine mesenchymal tumors that exhibit predominant variant morphologic features particularly of the myxoid nature currently appears less informative as there is extensive overlap of CD10, desmin, actin, h-caldesmon, ER, and PR among ESS, UUS, LMS, and IMT, all of which may show myxoid change. While cyclin D1 and ALK expression may suggest *YWHAE*-rearranged HG-ESS and IMT, respectively, robust immunohistochemical markers identifying other variants of ESS, including *BCOR*-rearranged HG-ESS, UUS, or myxoid LMS are currently lacking. Furthermore, case 3 reported herein showed diffuse cyclin D1 expression, further complicating the differential diagnosis with *YWHAE*-rearranged HG-ESS. All 3 of our *BCOR*-rearranged ESS showed strong and diffuse CD10 expression with limited desmin or SMA staining. This immunoprofile of a uterine sarcoma bearing resemblance to myxoid LMS, but extending from the endometrium and displaying tongue-like myometrial invasion should prompt molecular testing such as FISH or RNA sequencing. Akin to hematologic malignancies and soft tissue sarcomas, detection of specific genetic alterations by these methods will likely become pivotal in refining the diagnosis and classification of uterine mesenchymal tumors that display ambiguous morphologic and immunophenotypic features.

In summary, we highlight the histomorphologic features of *BCOR*-rearranged ESS, a distinct entity that should be considered in the differential diagnosis of myxoid uterine mesenchymal tumors. Given that the cytomorphologic features exceed that allowable for LG-ESS, in conjunction with the aggressive clinical behaviour suggested in our study and at least one other, *BCOR*-rearranged ESS are best classified as a form of HG-ESS distinct from *YWHAE*-rearranged ESS. With increasing awareness of this tumor type and its morphologic differential diagnosis, combined with the increasing availability of next-generation sequencing, it is likely that such cases will be more readily detected in the near future.

Acknowledgments

We would like to thank Bradley Quade and Lawrence C. Kenyon for their contribution in the review of these cases.

References

1. Kosary, CL. Cancer of the Corpus Uteri. In: Ries, LAG.Young, JL.Keel, GE., et al., editors. SEER Survival Monograph: Cancer Survival Among Adults: US SEER Program, 1988–2001, Patient and Tumor Characteristics. Bethesda, MD: National Cancer Institute; 2007. p. 123-132.SEER Program, NIH Pub. No. 07-6215
2. Norris HJ, Taylor HB. Mesenchymal tumors of the uterus: A clinical and pathological study of 53 endometrial stromal tumors. Cancer. 1966; 19:755–766. [PubMed: 5939046]
3. Lee CH, Nucci MR. Endometrial stromal sarcoma--the new genetic paradigm. Histopathology. 2015; 67:1–19. [PubMed: 25355621]
4. Ali RH, Rouzbahman M. Endometrial stromal tumours revisited: an update based on the 2014 WHO classification. J Clin Pathol. 2015; 68:325–332. [PubMed: 25595274]
5. Conklin CMJ, Longacre TA. Endometrial stromal tumors: the new WHO classification. Adv Anat Pathol. 2014; 21:383–393. [PubMed: 25299308]

6. Kurman, RJ., Carcangiu, ML., Herrington, CS., et al. World Health Organization Classification of Tumours of Female Reproductive Organs. Lyon, France: World Health Organization; 2014.
7. Chang KL, Crabtree GS, Lim-Tan SK, et al. Primary uterine endometrial stromal neoplasms. A clinicopathologic study of 117 cases. Am J Surg Pathol. 1990; 14:415–438. [PubMed: 2327549]
8. Evans HL. Endometrial stromal sarcoma and poorly differentiated endometrial sarcoma. Cancer. 1982; 50:2170–2182. [PubMed: 7127257]
9. Chew I, Oliva E. Endometrial stromal sarcomas: a review of potential prognostic factors. Adv Anat Pathol. 2010; 17:113–121. [PubMed: 20179433]
10. Baker PM, Moch H, Oliva E. Unusual morphologic features of endometrial stromal tumors: a report of 2 cases. Am J Surg Pathol. 2005; 29:1394–1398. [PubMed: 16160484]
11. Clement PB, Scully RE. Endometrial stromal sarcomas of the uterus with extensive endometrioid glandular differentiation: a report of three cases that caused problems in differential diagnosis. Int J Gynecol Pathol. 1992; 11:163–173. [PubMed: 1399225]
12. Fitko R, Brainer J, Schink JC, et al. Endometrial stromal sarcoma with rhabdoid differentiation. Int J Gynecol Pathol. 1990; 9:379–382. [PubMed: 1700973]
13. Huang HY, Ladanyi M, Soslow RA. Molecular detection of JAZF1-JJAZ1 gene fusion in endometrial stromal neoplasms with classic and variant histology: evidence for genetic heterogeneity. Am J Surg Pathol. 2004; 28:224–232. [PubMed: 15043312]
14. McCluggage WG, Date A, Bharucha H, et al. Endometrial stromal sarcoma with sex cord-like areas and focal rhabdoid differentiation. Histopathology. 1996; 29:369–374. [PubMed: 8910045]
15. McCluggage WG, Young RH. Endometrial stromal sarcomas with true papillae and pseudopapillae. Int J Gynecol Pathol. 2008; 27:555–561. [PubMed: 18753964]
16. Yilmaz A, Rush DS, Soslow RA. Endometrial stromal sarcomas with unusual histologic features: a report of 24 primary and metastatic tumors emphasizing fibroblastic and smooth muscle differentiation. Am J Surg Pathol. 2002; 26:1142–1150. [PubMed: 12218570]
17. Stadsvold JL, Molpus KL, Baker JJ, et al. Conservative management of a myxoid endometrial stromal sarcoma in a 16-year-old nulliparous woman. Gynecol Oncol. 2005; 99:243–245. [PubMed: 16054205]
18. Kim HS, Yoon G, Jung YY, et al. Fibromyxoid variant of endometrial stromal sarcoma with atypical bizarre nuclei. Int J Clin Exp Pathol. 2015; 8:3316–3321. [PubMed: 26045860]
19. Kasashima S, Kobayashi M, Yamada M, et al. Myxoid endometrial stromal sarcoma of the uterus. Pathol Int. 2003; 53:637–641. [PubMed: 14507323]
20. Regauer S, Emberger W, Reich O, et al. Cytogenetic analyses of two new cases of endometrial stromal sarcoma--non-random reciprocal translocation t(10;17)(q22;p13) correlates with fibrous ESS. Histopathology. 2008; 52:780–783. [PubMed: 18439162]
21. Stewart CJR, Leung YC, Murch A, et al. Evaluation of fluorescence in-situ hybridization in monomorphic endometrial stromal neoplasms and their histological mimics: a review of 49 cases. Histopathology. 2014; 65:473–482. [PubMed: 24592973]
22. Hwang H, Matsuo K, Duncan K, et al. Immunohistochemical panel to differentiate endometrial stromal sarcoma, uterine leiomyosarcoma and leiomyoma: something old and something new. J Clin Pathol. 2015; 68:710–717. [PubMed: 25991737]
23. Abeler VM, Nenodovic M. Diagnostic immunohistochemistry in uterine sarcomas: a study of 397 cases. Int J Gynecol Pathol. 2011; 30:236–243. [PubMed: 21464730]
24. McCluggage WG, Sumathi VP, Maxwell P. CD10 is a sensitive and diagnostically useful immunohistochemical marker of normal endometrial stroma and of endometrial stromal neoplasms. Histopathology. 2001; 39:273–278. [PubMed: 11532038]
25. Koontz JI, Soreng AL, Nucci M, et al. Frequent fusion of the JAZF1 and JJAZ1 genes in endometrial stromal tumors. Proc Natl Acad Sci USA. 2001; 98:6348–6353. [PubMed: 11371647]
26. Kurihara S, Oda Y, Ohishi Y, et al. Endometrial stromal sarcomas and related high-grade sarcomas: immunohistochemical and molecular genetic study of 31 cases. Am J Surg Pathol. 2008; 32:1228–1238. [PubMed: 18580489]
27. Nucci MR, Harburger D, Koontz J, et al. Molecular analysis of the JAZF1-JJAZ1 gene fusion by RT-PCR and fluorescence in situ hybridization in endometrial stromal neoplasms. Am J Surg Pathol. 2007; 31:65–70. [PubMed: 17197920]

28. Micci F, Panagopoulos I, Bjerkehagen B, et al. Consistent rearrangement of chromosomal band 6p21 with generation of fusion genes JAZF1/PHF1 and EPC1/PHF1 in endometrial stromal sarcoma. Cancer Res. 2006; 66:107–112. [PubMed: 16397222]
29. Micci F, Gorunova L, Gatius S, et al. MEA6/PHF1 is a recurrent gene fusion in endometrial stromal sarcoma. Cancer Lett. 2014; 347:75–78. [PubMed: 24530230]
30. Panagopoulos I, Micci F, Thorsen J, et al. Novel fusion of MYST/Esa1-associated factor 6 and PHF1 in endometrial stromal sarcoma. PloS One. 2012; 7:e39354. [PubMed: 22761769]
31. Dewaele B, Przybyl J, Quattrone A, et al. Identification of a novel, recurrent MBTD1-CXorf67 fusion in low-grade endometrial stromal sarcoma. Int J Cancer. 2014; 134:1112–1122. [PubMed: 23959973]
32. D'Angelo E, Ali RH, Espinosa I, et al. Endometrial stromal sarcomas with sex cord differentiation are associated with PHF1 rearrangement. Am J Surg Pathol. 2013; 37:514–521. [PubMed: 23211293]
33. Leath CA, Huh WK, Hyde J Jr, et al. A multi-institutional review of outcomes of endometrial stromal sarcoma. Gynecol Oncol. 2007; 105:630–634. [PubMed: 17320937]
34. Lee CH, Ou WB, Marino-Enriquez A, et al. 14-3-3 fusion oncogenes in high-grade endometrial stromal sarcoma. Proc Natl Acad Sci USA. 2012; 109:929–934. [PubMed: 22223660]
35. Halbwedl I, Ullmann R, Kremser ML, et al. Chromosomal alterations in low-grade endometrial stromal sarcoma and undifferentiated endometrial sarcoma as detected by comparative genomic hybridization. Gynecol Oncol. 2005; 97:582–587. [PubMed: 15863163]
36. Chiang S, Oliva E. Cytogenetic and molecular aberrations in endometrial stromal tumors. Hum Pathol. 2011; 42:609–617. [PubMed: 21420714]
37. Lee CH, Marino-Enriquez A, Ou W, et al. The clinicopathologic features of YWHAE-FAM22 endometrial stromal sarcomas: a histologically high-grade and clinically aggressive tumor. Am J Surg Pathol. 2012; 36:641–653. [PubMed: 22456610]
38. Lee CH, Ali RH, Rouzbahman M, et al. Cyclin D1 as a diagnostic immunomarker for endometrial stromal sarcoma with YWHAE-FAM22 rearrangement. Am J Surg Pathol. 2012; 36:1562–1570. [PubMed: 22982899]
39. Lee CH, Hoang L, Yip S, et al. Frequent expression of KIT in endometrial stromal sarcoma with YWHAE genetic rearrangement. Mod Pathol. 2014; 27:751–757. [PubMed: 24186140]
40. Sciallis AP, Bedroske PP, Schoolmeester JK, et al. High-grade endometrial stromal sarcomas: a clinicopathologic study of a group of tumors with heterogenous morphologic and genetic features. Am J Surg Pathol. 2014; 38:1161–1172. [PubMed: 25133706]
41. Cheng DT, Mitchell TN, Zehir A, et al. Memorial Sloan Kettering-Integrated Mutation Profiling of Actionable Cancer Targets (MSK-IMPACT): A Hybridization Capture-Based Next-Generation Sequencing Clinical Assay for Solid Tumor Molecular Oncology. J Mol Diagn. 2015; 17:251–264. [PubMed: 25801821]
42. Zheng Z, Liebers M, Zhelyazkova B, et al. Anchored multiplex PCR for targeted next-generation sequencing. Nat Med. 2014; 20:1479–1484. [PubMed: 25384085]
43. Antonescu CR, Sung YS, Chen C, et al. Novel ZC3H7B-BCOR, MEAF6-PHF1, and EPC1-PHF1 fusions in ossifying fibromyxoid tumors--molecular characterization shows genetic overlap with endometrial stromal sarcoma. Genes Chromosomes Cancer. 2014; 53:183–193. [PubMed: 24285434]
44. Antonescu CR, Zhang L, Chang NE, et al. EWSR1-POU5F1 fusion in soft tissue myoepithelial tumors. A molecular analysis of sixty-six cases, including soft tissue, bone, and visceral lesions, showing common involvement of the EWSR1 gene. Genes Chromosomes Cancer. 2010; 49:1114–1124. [PubMed: 20815032]
45. Panagopoulos I, Thorsen J, Gorunova L, et al. Fusion of the ZC3H7B and BCOR genes in endometrial stromal sarcomas carrying an X;22-translocation. Genes Chromosomes Cancer. 2013; 52:610–618. [PubMed: 23580382]
46. Abeler VM, Røyne O, Thoresen S, et al. Uterine sarcomas in Norway. A histopathological and prognostic survey of a total population from 1970 to 2000 including 419 patients. Histopathology. 2009; 54:355–364. [PubMed: 19236512]

47. King ME, Dickersin GR, Scully RE. Myxoid leiomyosarcoma of the uterus. A report of six cases. Am J Surg Pathol. 1982; 6:589–598. [PubMed: 7180961]
48. Parra-Herran C, Schoolmeester JK, Yuan L, et al. Myxoid Leiomyosarcoma of the Uterus: A Clinicopathologic Analysis of 30 Cases and Review of the Literature With Reappraisal of Its Distinction From Other Uterine Myxoid Mesenchymal Neoplasms. Am J Surg Pathol. 2016; 40:285–301. [PubMed: 26866354]
49. Leitao MM, Sonoda Y, Brennan MF, et al. Incidence of lymph node and ovarian metastases in leiomyosarcoma of the uterus. Gynecol Oncol. 2003; 91:209–212. [PubMed: 14529683]
50. Kapp DS, Shin JY, Chan JK. Prognostic factors and survival in 1396 patients with uterine leiomyosarcomas: Emphasis on impact of lymphadenectomy and oophorectomy. Cancer. 2008; 112:820–830. [PubMed: 18189292]
51. Dos Santos LA, Garg K, Diaz JP, et al. Incidence of lymph node and adnexal metastasis in endometrial stromal sarcoma. Gynecol Oncol. 2011; 121:319–322. [PubMed: 21276609]
52. Oliva E, Young RJ, Clement PB, et al. Myxoid and fibrous endometrial stromal tumors of the uterus: a report of 10 cases. Int J Gynecol Pathol. 1999; 18:310–319. [PubMed: 10542938]
53. Huynh KD, Fischle W, Verdin E, et al. BCoR, a novel corepressor involved in BCL-6 repression. Genes Dev. 2000; 14:1810–1823. [PubMed: 10898795]
54. Yamamoto Y, Abe A, Emi N. Clarifying the impact of polycomb complex component disruption in human cancers. Mol Cancer Res. 2014; 12:479–484. [PubMed: 24515802]
55. Simon JA, Kingston RE. Mechanisms of polycomb gene silencing: knowns and unknowns. Nat Rev Mol Cell Biol. 2009; 10:697–708. [PubMed: 19738629]
56. Wamstad JA, Corcoran CM, Keating AM, et al. Role of the transcriptional corepressor Bcor in embryonic stem cell differentiation and early embryonic development. PloS One. 2008; 3:e2814. [PubMed: 18795143]
57. Fan Z, Yamaza T, Lee JS, et al. BCOR regulates mesenchymal stem cell function by epigenetic mechanisms. Nat Cell Biol. 2009; 11:1002–1009. [PubMed: 19578371]
58. Cao Q, Gearhart MD, Gery S, et al. BCOR regulates myeloid cell proliferation and differentiation. Leukemia. 2006; 30:1155–1165.
59. Yang JA, Tubo NJ, Gearhart MD, et al. Cutting edge: Bcl6-interacting corepressor contributes to germinal center T follicular helper cell formation and B cell helper function. J Immunol. 2015; 194:5604–5608. [PubMed: 25964495]
60. Hilton EN, Manson FD, Urquhart JE, et al. Left-sided embryonic expression of the BCL-6 corepressor, BCOR, is required for vertebrate laterality determination. Hum Mol Genet. 2007; 16:1773–1782. [PubMed: 17517692]
61. Sakano D, Kato A, Parikh N, et al. BCL6 canalizes Notch-dependent transcription, excluding Mastermind-like1 from selected target genes during left-right patterning. Dev Cell. 2010; 18:450–462. [PubMed: 20230751]
62. Ng D, Thakker N, Cororan CM. Oculofaciocardiodental and Lenz microphthalmia syndromes result from distinct classes of mutations in BCOR. Nat Genet. 2004; 36:411–416. [PubMed: 15004558]
63. Grossmann V, Tiacci E, Holmes AB, et al. Whole-exome sequencing identifies somatic mutations of BCOR in acute myeloid leukemia with normal karyotype. Blood. 2011; 118:6153–6163. [PubMed: 22012066]
64. Lindsley RC, Mar BG, Mazzola E, et al. Acute myeloid leukemia ontogeny is defined by distinct somatic mutations. Blood. 2015; 125:1367–1376. [PubMed: 25550361]
65. Damm F, Chesnais V, Nagata Y, et al. BCOR and BCORL1 mutations in myelodysplastic syndromes and related disorders. Blood. 2013; 122:3169–3177. [PubMed: 24047651]
66. Kulasekararaj AG, Jiang J, Smith AE, et al. Somatic mutations identify a subgroup of aplastic anemia patients who progress to myelodysplastic syndrome. Blood. 2014; 124:2698–2704. [PubMed: 25139356]
67. Dobashi A, Tsuyama N, Asaka R, et al. Frequent BCOR Aberrations in Extranodal NK/T-Cell Lymphoma, Nasal Type. Genes Chromosomes Cancer. 2016; 55:460–471. [PubMed: 26773734]

68. Lee S, Park HY, Kang SY, et al. Genetic alterations of JAK/STAT cascade and histone modification in extranodal NK/T-cell lymphoma nasal type. Oncotarget. 2015; 6:17764–17776. [PubMed: 25980440]
69. Zhang J, Benavente CA, McEvoy J, et al. A novel retinoblastoma therapy from genomic and epigenetic analyses. Nature. 2012; 481:329–334. [PubMed: 22237022]
70. Pugh TJ, Weeraratne SD, Archer TC, et al. Medulloblastoma exome sequencing uncovers subtype-specific somatic mutations. Nature. 2012; 488:106–110. [PubMed: 22820256]
71. Sturm D, Orr BA, Toprak UH, et al. New Brain Tumor Entities Emerge from Molecular Classification of CNS-PNETs. Cell. 2016; 164:1060–1072. [PubMed: 26919435]
72. Shern JF, Chen L, Chmielecki J, et al. Comprehensive genomic analysis of rhabdomyosarcoma reveals a landscape of alterations affecting a common genetic axis in fusion-positive and fusion-negative tumors. Cancer Discov. 2014; 4:216–231. [PubMed: 24436047]
73. Astolfi A, Melchionda F, Perotti D, et al. Whole transcriptome sequencing identifies BCOR internal tandem duplication as a common feature of clear cell sarcoma of the kidney. Oncotarget. 2015; 6:40934–40939. [PubMed: 26516930]
74. Karlsson J, Valind A, Gisselsson D. BCOR internal tandem duplication and YWHAE-NUTM2B/E fusion are mutually exclusive events in clear cell sarcoma of the kidney. Genes Chromosomes Cancer. 2016; 55:120–123. [PubMed: 26493387]
75. Roy A, Kumar V, Zorman B, et al. Recurrent internal tandem duplications of BCOR in clear cell sarcoma of the kidney. Nat Commun. 2015; 6:8891. [PubMed: 26573325]
76. Ueno-Yokohata H, Okita H, Nakasato K, et al. Consistent in-frame internal tandem duplications of BCOR characterize clear cell sarcoma of the kidney. Nat Genet. 2015; 47:861–863. [PubMed: 26098867]
77. Specht K, Zhang L, Sung YS, et al. Novel BCOR-MAML3 and ZC3H7B-BCOR Gene Fusions in Undifferentiated Small Blue Round Cell Sarcomas. Am J Surg Pathol. 2016; 40:433–442. [PubMed: 26752546]
78. Cohen-Gogo S, Cellier C, Coindre JM, et al. Ewing-like sarcomas with BCOR-CCNB3 fusion transcript: a clinical, radiological and pathological retrospective study from the Société Française des Cancers de L'Enfant. Pediatr Blood Cancer. 2014; 61:2191–2198. [PubMed: 25176412]
79. Pierron G, Tirode F, Lucchesi C, et al. A new subtype of bone sarcoma defined by BCOR-CCNB3 gene fusion. Nat Genet. 2012; 44:461–466. [PubMed: 22387997]
80. Yamamoto Y, Tsuzuki S, Tsuzuki M, et al. BCOR as a novel fusion partner of retinoic acid receptor alpha in a t(X;17)(p11;q12) variant of acute promyelocytic leukemia. Blood. 2010; 116:4274–4283. [PubMed: 20807888]
81. Harb M, Becker MM, Vitour D, et al. Nuclear localization of cytoplasmic poly(A)-binding protein upon rotavirus infection involves the interaction of NSP3 with eIF4G and RoXaN. J Virol. 2008; 82:11283–11293. [PubMed: 18799579]
82. Vitour D, Lindenbaum P, Vende P, et al. RoXaN, a novel cellular protein containing TPR, LD, and zinc finger motifs, forms a ternary complex with eukaryotic initiation factor 4G and rotavirus NSP3. J Virol. 2004; 78:3851–3862. [PubMed: 15047801]
83. Kibar Y, Aydin A, Deniz H, et al. A rare case of low-grade endometrial stromal sarcoma with myxoid differentiation and atypical bizarre cells. Eur J Gynaecol Oncol. 2008; 29:397–398. [PubMed: 18714579]
84. Park JY, Sung CO, Jang SJ, et al. Pulmonary metastatic nodules of uterine low-grade endometrial stromal sarcoma: histopathological and immunohistochemical analysis of 10 cases. Histopathology. 2013; 63:833–840. [PubMed: 24024590]

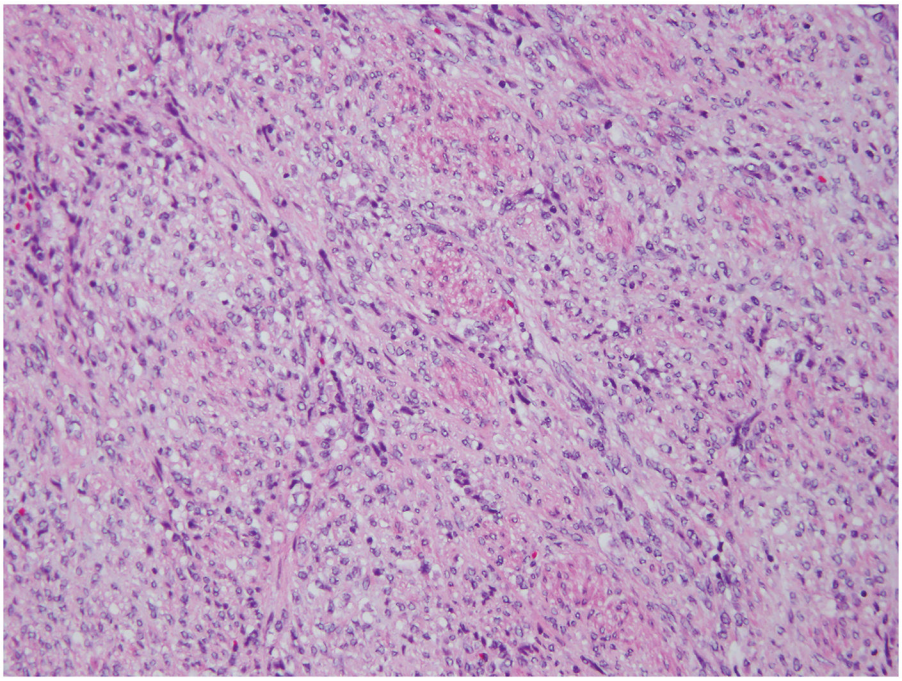

Figure 1. Histopathology of t(X;22) *ZC3H7B-BCOR* ESS, case 1

The tumor was spindled with epithelioid areas, showed focal fascicular architecture and extensive myxoid change. The tumor cell nuclei were enlarged, with irregular nuclear contours and displayed clear to hyperchromatic chromatin.

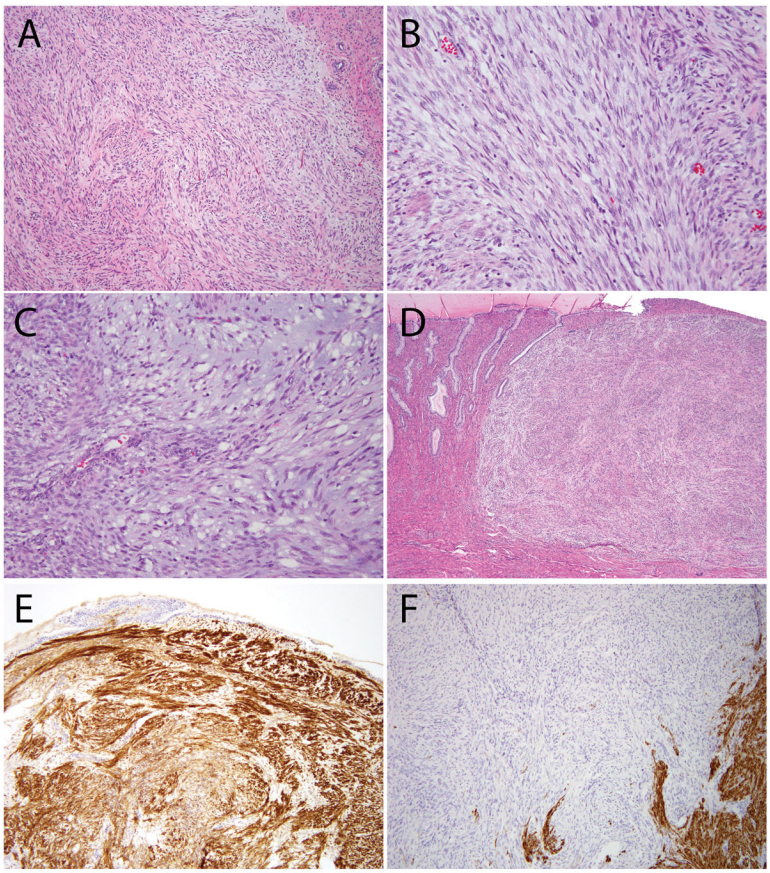

Figure 2. Additional histologic features of ESS with *ZC3H7B-BCOR* translocation, case 1

(A) Predominantly spindled neoplasm with myxoid features and a pushing border; (B) Focal fascicular architecture and thin-walled blood vessels; (C) Areas with more prominent myxoid stroma; (D) Involvement of the uterine cervix; (E) CD10 was strongly positive; (F) Desmin was negative (positive staining seen in background myometrium).

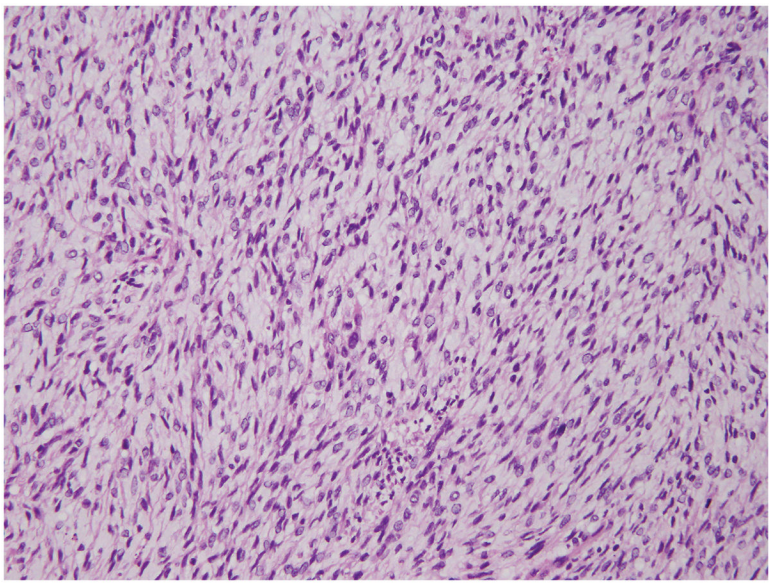

Figure 3. Histopathology of t(X;22) *ZC3H7B-BCOR* ESS, case 2

The tumor was composed of spindled and epithelioid cells with extensive myxoid changes. The tumor cell nuclei were monotonous, and the chromatin varied from pale/clear to hyperchromatic.

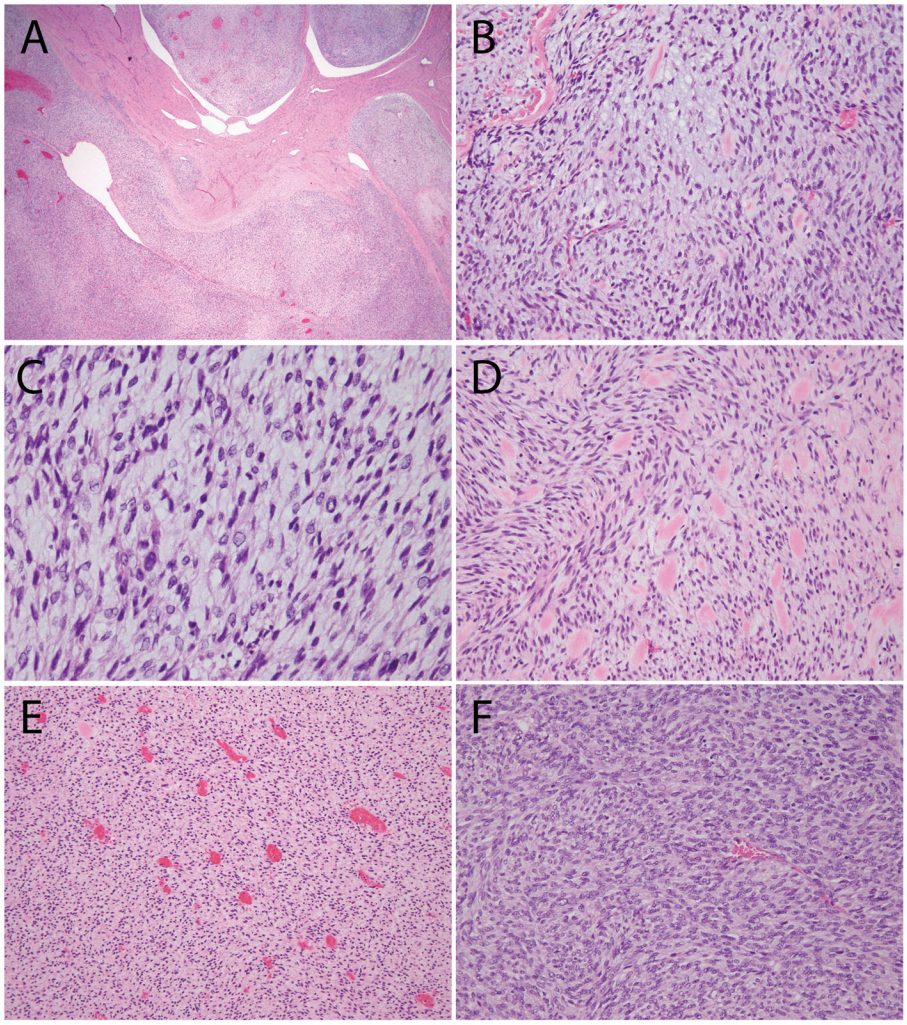

Figure 4. Additional histologic features of ESS with *ZC3H7B-BCOR* translocation, case 2

(A) Tongue-like myoinvasion and worm-like plugs of the uterine vessels; (B) Spindled cells embedded in myxoid stroma; (C) Cytologic atypia with enlarged nuclei, irregular nuclear contours and hyperchromatic to pale/clear chromatin; (D) Collagen plaques; (E) Thin-walled blood vessels; (F) More cellular areas were present with less myxoid stroma.

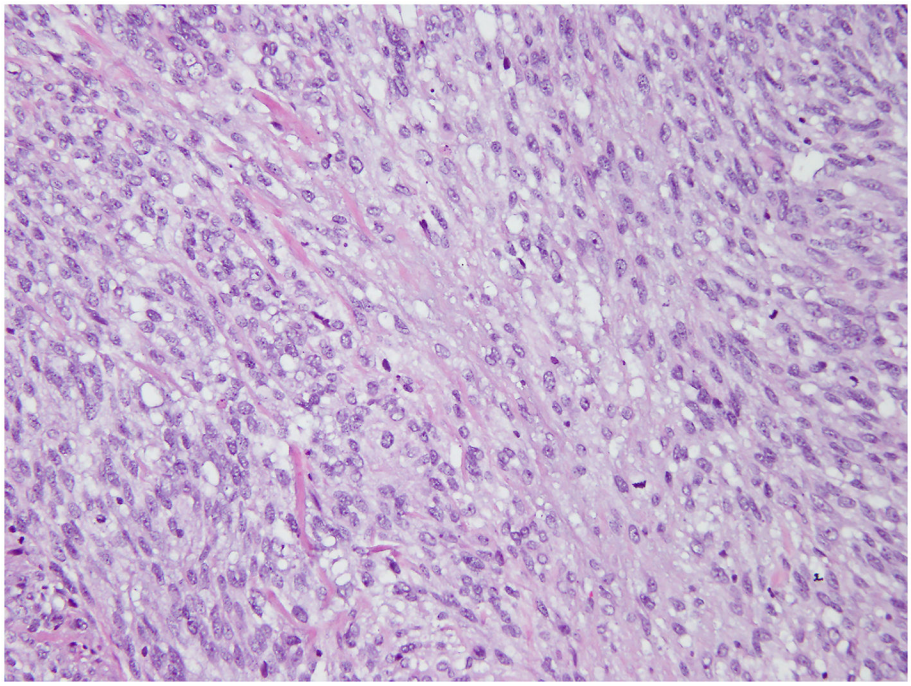

Figure 5. Histopathology of t(X;22) *ZC3H7B-BCOR* ESS, case 3

The tumor was composed of spindled cells in a background diffuse myxoid stroma. The tumor cell nuclei were enlarged, had irregular nuclear contours, coarse chromatin and some had conspicuous nucleoli. Mitoses were up to 10/10 high power fields.

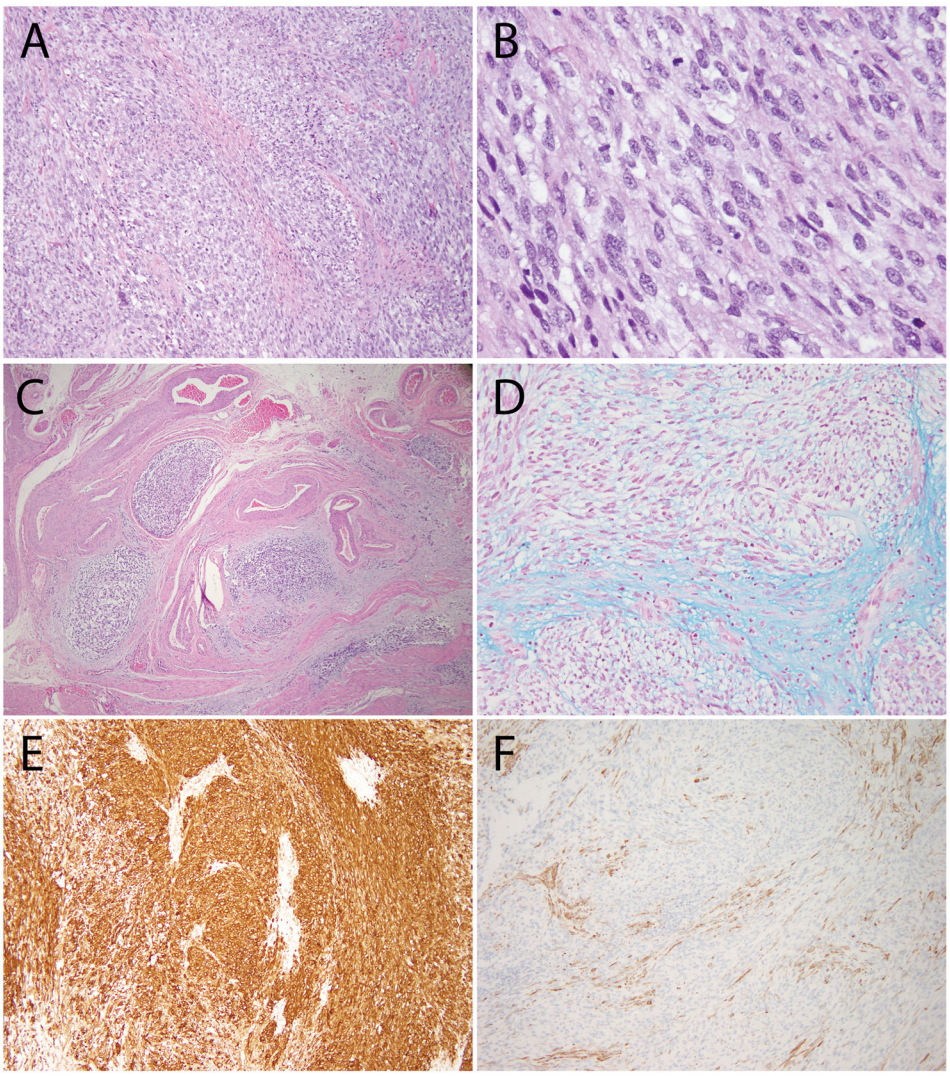

Figure 6. Additional histologic features of ESS with *ZC3H7B-BCOR* translocation, case 3

(A–B) The tumor was composed of spindled cells in a myxoid stroma; (C) Worm-like plugs of tumor were seen in blood vessels; (D) Alcian blue pH 2.5 was positive; (E) CD10 was strongly and diffusely positive; (F) Caldesmon was negative (positive staining seen in background myometrium).

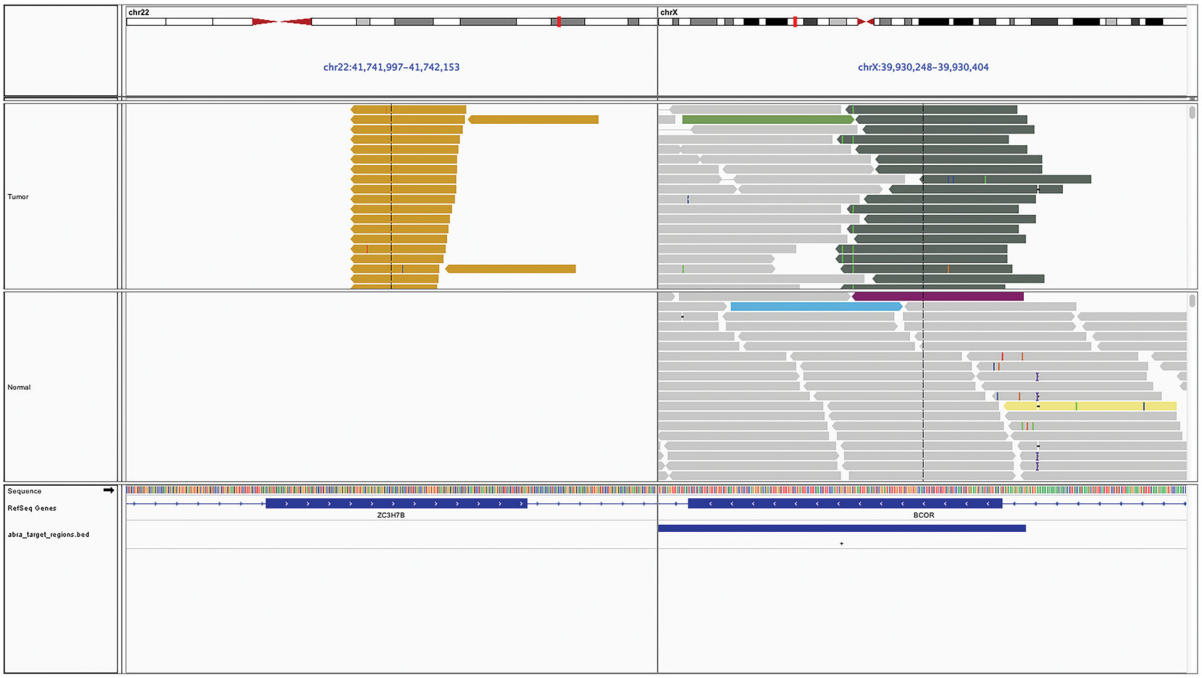

Figure 7. Pictorial representation of the *ZC3H7B-BCOR* translocation on Integrated Genome Viewer

Each bar is a single sequenced read with the top panel displaying data from tumor sample and bottom panel displaying its matched normal sample. The reads are sorted to highlight read pairs with discordant read mapping on the top for each sample. As evident, one set of reads maps to *ZC3H7B* on chromosome 22 while the their corresponding paired end reads map to *BCOR* on the X chromosome, supporting the presence of a somatic fusion involving both genes.

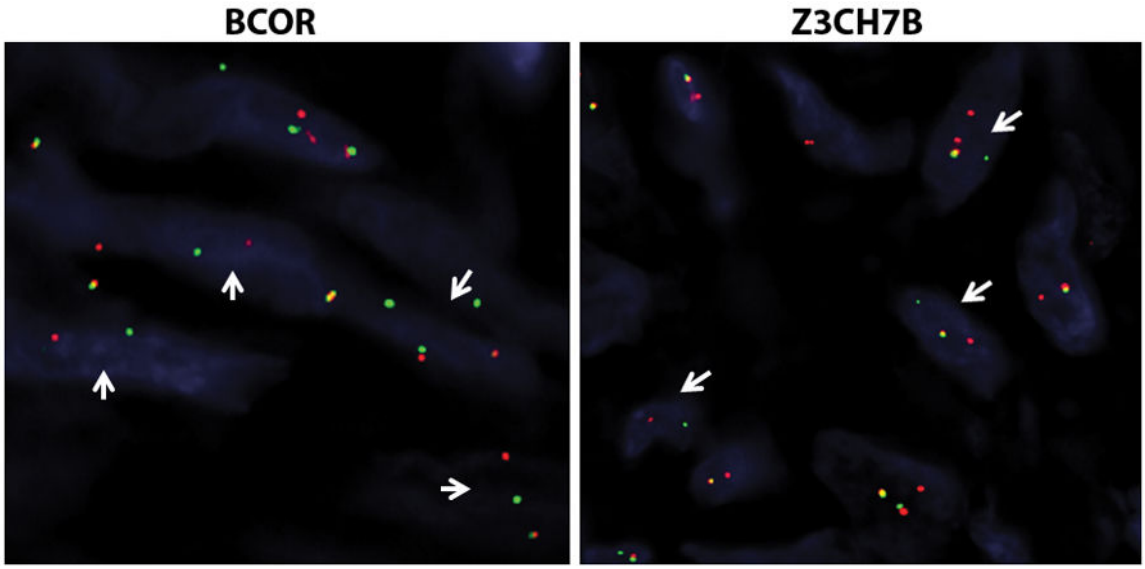

Figure 8. Fluorescence in-situ hybridization confirmation of *BCOR* and *ZC3H7B* rearrangements in ESS case 1

Break-apart assays for *BCOR* and *ZC3H7B* both show split signals (arrows, red probe centromeric, green probe telomeric) confirming rearrangements in both genes.